

Large zenith angle observation of the PeVatron candidate SNR G106.3+2.7 with the LST-1 and the MAGIC telescopes.

Marie-Sophie Carrasco,^{a,*} C. Arcaro,^b M. de Bony,^a F. Cassol,^a Y. Chai,^c H. Costantini,^a G. Emery,^d L. Feligioni,^a M. Pihet^d and T. Saito^c on behalf of the CTAO-LST Project and the MAGIC Collaboration

^aAix Marseille Univ, CNRS/IN2P3, CPPM,
Marseille, France

^bINFN,
Padova, Italy

^cICRR,
Tokyo, Japan

^dIAA,
Granada, Spain

E-mail: carrasco@cppm.in2p3.fr

Imaging Atmospheric Cherenkov Telescopes (IACTs) are ideal for investigating the nature of moderately extended gamma-ray sources at very high energy thanks to their optimal angular and energy resolution compared to ground array detectors. The Supernova Remnant SNR G106.3+2.7 is one of the most promising Galactic hadronic PeVatron candidates. We carried out observations using the Large-Sized Telescope prototype (LST-1) of the Cherenkov Telescope Array Observatory (CTAO) and the two neighboring IACTs of the MAGIC experiment at large zenith angle (LZA) to enhance the effective area at energies above tens of TeV. Data reconstruction and analysis are challenging due to the increased atmospheric depth and strong dependency on the zenith angle of the image properties. Therefore, specialized LZA reconstruction and analysis tools have been developed. We present a joint analysis of data from several telescope combinations, based on currently available statistics, including a preliminary study of the energy-dependent morphology and spectral models.

39th International Cosmic Ray Conference (ICRC2025)
15–24 July 2025
Geneva, Switzerland



*Speaker

1. Introduction

SNR G106.3+2.7 is a supernova remnant (SNR) recently confirmed to be a PeVatron by LHAASO, which measured emissions up to ~ 600 TeV [1, 2]. In radio it has the shape of a comet, characterized by a head with higher brightness and a fainter elongated tail [3]. The head region is colliding with a dense HI cloud and appears to contain the energetic pulsar (PSR) PSR J2229+6114 and its associated pulsar wind nebula (PWN), also known as the Boomerang Nebula. The tail region is expanding in a low density HI cavity, located in the vicinity of a dense molecular cloud [4].

Due to LHAASO's poor angular resolution and the complex nature of the SNR, the origin of the Ultra High Energy (UHE, $E \geq 100$ TeV) emission remains unknown. If the gamma-rays with energy above 100 TeV are associated with the head region, the PeVatron nature of the region could be associated with efficient leptonic acceleration in the PSR or PWN. If this signal instead originates in the tail region, it would indicate the presence of PeV hadrons accelerated in the SNR and possibly interacting with the nearby dense molecular cloud. The source, discovered in the early 90's [5], has been subject to extensive multi-wavelength (MWL) campaigns [6–11]. So far, no MWL spectral analysis was able to determine the leptonic or hadronic nature of SNR G106.3+2.7. Hadronic emission models tend to be favored, but the leptonic scenario has not been ruled out. Recently, MAGIC presented results which indicate energy dependent emission morphology at Very High Energy (VHE, $E \geq 1$ TeV) [12]. We aim to investigate these results with equivalent angular resolution but increased detection efficiency at energies above 10 TeV, which is achieved with Large Zenith Angle (LZA) pointing and with joint LST-1 and MAGIC observations.

2. LZA observation with LST-1 and MAGIC

SNR G106.3+2.7 is undergoing a multi-year observation campaign with LST-1 and the MAGIC telescopes, both located at the Observatorio del Roque de los Muchachos, La Palma (Canary Islands, Spain). LST-1, the Large-Sized Telescope prototype for the Cherenkov Telescope Array Observatory (CTAO), is optimized for gamma rays from ~ 20 GeV to a few TeV. MAGIC (Major Atmospheric Gamma Imaging Cherenkov Telescopes) is an array comprising two IACTs operational since 2003 and 2009, covering an energy range from ~ 50 GeV up to ≥ 100 TeV.

The final dataset will be a combination of mono LST-1, stereo MAGIC and joint stereo LST-1+MAGIC datasets. The joint stereo LST-1+MAGIC dataset is obtained with a simultaneous pointing to the source and a joint data reconstruction. Images are connected by a software trigger, which requires at least two telescope images per event. The source is observed in wobble mode, with two pointings positioned in a way to study both the head and the tail regions. The pointing is in the zenith range 55° - 75° , which allows for an increase in the effective area by a factor 3 at 10 TeV and up to 7 at 50 TeV. The angular resolution is below 0.1° for energies sufficiently above the analysis threshold, which depends on the zenith pointing.

3. Data analysis

The mono LST-1, stereo MAGIC and joint stereo LST-1+MAGIC datasets are reconstructed with their respective pipelines: *lstchain*, *MARS* and *magic-cta-pipe* [13–15]. The Random Forests

used for reconstruction were trained on Monte-Carlo data simulated along the source declination line with a dense grid of pointings in order to reduce biases arising from rapidly varying shower parameters at large zenith angles. The high level analysis was performed with `gammapy` [16].

In this work, we present preliminary results obtained with 42.6 hours of the mono LST-1 dataset, in the energy range 3-100 TeV. We first present skymaps of the source in several energy bins, then we perform the spectral modeling of the source (1D analysis) in the same regions of interest (ROIs) used by MAGIC or LHAASO, and finally we perform a spectral and morphological modeling of the source (3D analysis) over the whole FoV. Additionally, we perform a joint 1D analysis of this dataset with the middle zenith angle dataset (120 hrs) used for the MAGIC 2023 publication [12], which permits to show the coherence of recent LZA results with data taken with different pointing conditions and in a different energy range.

3.1 Background model estimation

The study of extended sources demands to correctly estimate the residual hadronic background to be subtracted from the detected signal. For that, it is necessary to estimate the background instrument response function (IRF), which describes the telescope acceptance for gamma-like protons over the field of view (FoV), which is 4.5° of diameter for LST-1 and 3.5° for MAGIC. At LZA the rapidly changing atmosphere depth implies an inhomogeneous acceptance in the FoV also in the case of a single telescope. The background IRF estimation was performed with the `BAccMod` package¹ by creating an acceptance model from the stacked data properly masked in the source region. More precisely, each dataset was binned in zenith, and a 3D acceptance model (energy, pointing altitude and azimuth) was produced for each zenith bin by stacking the counts and normalizing them to get the background rates in FoV coordinates. For the LST-1 mono dataset specifically, we handled the lack of statistics by fitting an analytical function to the data. The spatial acceptance is described by a 2D gaussian function with two linear gradients along the altitude and azimuth axis to account for the zenith dependent variation over the FoV. The background IRF was then used in the ring background method [17] provided by `gammapy`. This method allowed us to get a good background model from 3 to 100 TeV for the LST-1 dataset, and from 0.5 to 20 TeV for the MAGIC 2023 dataset.

3.2 Spectral analysis (1D analysis)

The spectral analysis was performed considering ON regions from published results: the head and tail ROIs from MAGIC 2023, and the r_{39} extension of the LHAASO WCDA source [2, 12]. The emission spectrum was modeled with a power law (PL) function given by $\frac{dN}{dE} = N_0 \left(\frac{E}{3\text{TeV}}\right)^{-\Gamma}$. The spectral points were computed requiring a minimum of 2σ significance.

3.3 Spectral and spatial analysis (3D analysis)

The 3D analysis was performed by fitting a set of spatial models (point-like, 1D or 2D Gaussian, disk, and ellipse) and spectral models (PL, PL with exponential cut-off (ECPL), and log-parabola (LP)). Considering the possibilities of the absence of a source or the presence of one or two sources,

¹<https://github.com/mdebony/BAccMod>

we fitted a total of 256 model combinations. The source models were initialized with the parameters of the head and/or tail results from MAGIC.

The best fit models were selected by using the Wilk's theorem. The best non-nested models were then ranked according to the Akaike Information Criterion (AIC) [18, 19]. First, we computed the significance for each set of nested models to create a significance matrix $\mathbf{S} = (s_{ij})$, where s_{ij} is the entry giving the significance of the model M_j when tested as an alternative to the null model M_i . Then, the models were filtered with a 3σ significance threshold: a model M_j was rejected if a null model M_i existed such as $S_{ij} < 3\sigma$, or if an alternative model M_k existed such as $S_{jk} \geq 3\sigma$. The AIC score was then computed for each remaining non-nested model. The best-fit model was determined as the one with the minimum AIC score. Models presenting a score difference $\Delta\text{AIC} \leq 2$ were considered compatible. Any model with $\Delta\text{AIC} > 2$ is considered rejected. The spatial residuals of each model were checked for final validation.

3.4 Analysis parameters

We masked the source with two 0.4° circle regions centered on the MAGIC head and tail positions. This mask was applied for the acceptance and the ring background modeling. The ring kernel had a 0.12° internal radius and a 0.5° external radius. The significance was computed with a 0.12° correlation radius.

4. Results

4.1 Energy-dependent morphology

Fig. 1 shows the significance map of the Boomerang SNR region obtained with 42.6 hours of LZA observation with LST-1, from 3 to 100 TeV. We see an extended region with more than 5σ significance extending over the whole SNR region, with a global maximum peak at 7.3σ in the tail region. Looking at the energy-dependent morphology, we can study the 3-6 TeV, 6-10 TeV, 10-50 TeV and 50-100 TeV energy bins. In these energy bins, we have a PSF ranging from 0.11° to 0.08° . A shift of the high-energy emission is observed from the head towards the tail, consistent with the one seen by MAGIC 2023. Hints of signal are also observed above 50 TeV in the outer tail region.

4.2 Spectral analysis (1D analysis)

Results from LST-1 are consistent with both the MAGIC and the LHAASO spectral studies. The increased statistics at higher energy coming from the LST-1 data, seems to soften the MAGIC spectral shape in the tail region. Furthermore, the addition of MAGIC 2023 data allows to better constrain the fit at lower energies.

4.3 Spectral and spatial analysis (3D analysis)

The best-fit result from the 3D analysis on LST-1 data is a model consisting of two extended sources with PL spectral emissions. The first source is described by a 1D Gaussian spatial model located on the same axis as the MAGIC regions, at the outer end of the tail region, towards the molecular cloud. Its hard PL spectral emission is consistent with the one measured in the MAGIC tail region. The second source is a large disk-like source, overlapping the LHAASO WCDA

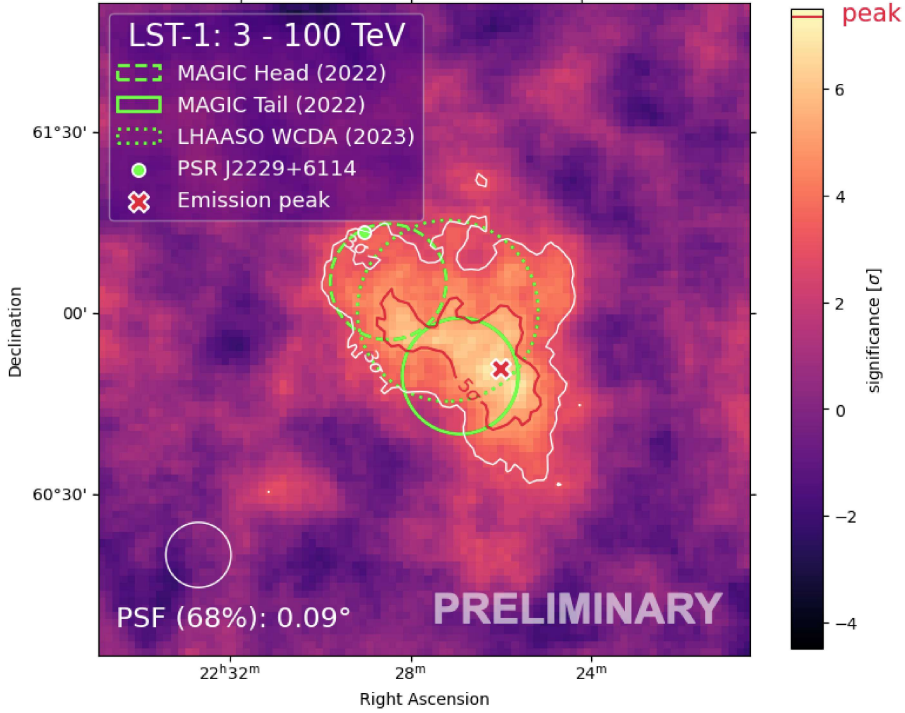


Figure 1: Significance map of the Boomerang SNR region obtained with 42.6 hours of LZA observation with LST-1. The position of the pulsar PSR J2229+6114, the head and tail ROIs from MAGIC and the LHAASO WCDA source radius are plotted in green for reference (dashed, full and dotted lines respectively). Significance contours at the 3σ (white) and 5σ (red) levels are overlaid. The global maximum significance peak (red cross) is at 7.3σ in the tail region. The white circle shows the gaussian kernel consistent with our PSF 68% containment radius evaluated at the energy center of the stacked dataset.

emission region, the MAGIC head region and almost the whole MAGIC tail region. The soft PL spectral emission is consistent with the one from the LHAASO WCDA source.

Two other models were discarded by the AIC: a very similar one with a disk-like source on the tail region instead of a 1D Gaussian ($\Delta\text{AIC} \approx 5$), and a single 2D Gaussian source model extending over the whole SNR region, with a PL spectrum consistent with LHAASO WCDA and KM2A ($\Delta\text{AIC} \approx 9$). The spatial residuals were good for both of these models.

5. Conclusions

SNR G106.3+2.7 is undergoing a multi-year observation campaign at LZA with LST-1 and MAGIC telescopes. We performed a preliminary analysis on a total of 42.6 hours of LST-1 data taken with a zenith angle between 55° and 75° . We detected the source at 5σ over the head and tail regions, with a global maximum emission peak in the tail. The energy-dependent morphology shows an apparent shift of the emission site towards the tail, with indications of emission above 50 TeV in the outer tail region. Both energy-dependent morphology and spectral analysis preliminary results were consistent with MAGIC and LHAASO's results. The spectral morphological analysis favored a model with two extended sources. The first source is a large disk-like source with a soft

PL spectral emission over the LHAASO WCDA, MAGIC head and part of MAGIC tail regions. The second source is a smaller 1D Gaussian source with a hard PL spectral emission, located in the outer tail region. The joint observation campaign is ongoing and joint LST-1 and MAGIC results will be available soon.

References

- [1] Z. Cao, F.A. Aharonian, Q. An, Axikegu, L.X. Bai, Y.X. Bai et al., *Ultrahigh-energy photons up to 1.4 petaelectronvolts from 12 -ray Galactic sources*, *Nature* **594** (2021) 33.
- [2] Z. Cao, F. Aharonian, Q. An, Y. Bai, Y. Bao, D. Bastieri et al., *The first lhaaso catalog of gamma-ray sources*, *The Astrophysical Journal Supplement Series* **271** (2024) 25.
- [3] R. Kothes, B. Uyaniker and S. Pineault, *The Supernova Remnant G106.3+2.7 and Its Pulsar-Wind Nebula: Relics of Triggered Star Formation in a Complex Environment*, *The Astrophysical Journal* **560** (2001) 236.
- [4] C. Ge, R.-Y. Liu, S. Niu, Y. Chen and X.-Y. Wang, *Revealing a peculiar supernova remnant G106.3+2.7 as a petaelectronvolt proton accelerator with X-ray observations*, *The Innovation* **2** (2021) .
- [5] G. Joncas and L.A. Higgs, *The DRAO galactic-plane survey. II. Field at $l=105.$* , *Astronomy and Astrophysics Supplement Series* **82** (1990) 113.
- [6] A. Albert, R. Alfaro, C. Alvarez, J.R.A. Camacho, J.C. Arteaga-Velázquez, K.P. Arunbabu et al., *HAWC J2227+610 and Its Association with G106.3+2.7, a New Potential Galactic PeVatron*, *The Astrophysical Journal Letters* **896** (2020) L29.
- [7] M. Amenomori, Y.W. Bao, X.J. Bi, D. Chen, T.L. Chen, W.Y. Chen et al., *Potential PeVatron supernova remnant G106.3+2.7 seen in the highest-energy gamma rays*, *Nature Astronomy* **5** (2021) 460.
- [8] A. De Sarkar, W. Zhang, J. Martín, D.F. Torres, J. Li and X. Hou, *LHAASO J2226+6057 as a pulsar wind nebula*, Sept., 2022.
- [9] Q.-C. Liu, P. Zhou and Y. Chen, *IRAM 30 m CO-line Observation toward the PeVatron Candidate G106.3+2.7: Direct Interaction between the Shock and the Molecular Cloud Remains Uncertain*, *The Astrophysical Journal* **926** (2022) 124.
- [10] K. Fang, M. Kerr, R. Blandford, H. Fleischhack and E. Charles, *Evidence for PeV Proton Acceleration from Fermi-LAT Observations of SNR G106.3+2.7*, *Physical Review Letters* **129** (2022) 071101.
- [11] I. Pope, K. Mori, M. Abdelmaguid, J.D. Gelfand, S.P. Reynolds, S. Safi-Harb et al., *A multi-wavelength investigation of PSR J2229+6114 and its pulsar wind nebula in the radio, X-ray, and gamma-ray bands*, Oct., 2023. 10.48550/arXiv.2310.04512.

- [12] H. Abe, S. Abe, V.A. Acciari, I. Agudo, T. Aniello, S. Ansoldi et al., *MAGIC observations provide compelling evidence of hadronic multi-TeV emission from the putative PeVatron SNR G106.3+2.7*, *Astronomy & Astrophysics* **671** (2023) A12.
- [13] R. López-Coto, A. Baquero, M.I. Bernardos, F. Cassol, L. Foffano, E. García et al., *lstchain: An analysis pipeline for lst-1, the first prototype large-sized telescope of cta*, in *30th Astronomical Data Analysis Software and Systems*, vol. 532, p. 357, Astronomical Society of the Pacific, 2020.
- [14] R. Zanin, E. Carmona, J. Sitarek, P. Colin, K. Frantzen, M. Gaug et al., *Mars, the magic analysis and reconstruction software*, in *Proc. of the 33rd International Cosmic Ray Conference, Rio de Janeiro, Brasil*, 2013.
- [15] H. Abe, K. Abe, S. Abe, V. Acciari, A. Aguasca-Cabot, I. Agudo et al., *Performance of the joint lst-1 and magic observations evaluated with crab nebula data*, *Astronomy & astrophysics* **680** (2023) A66.
- [16] C. Deil, R. Zanin, J. Lefaucheur, C. Boisson, B. Khélifi, R. Terrier et al., *Gammapy-a prototype for the cta science tools*, *arXiv preprint arXiv:1709.01751* (2017).
- [17] H. Abdalla, A. Abramowski, F. Aharonian, F.A. Benkhali, E. Angüner, M. Arakawa et al., *The hess galactic plane survey*, *Astronomy & Astrophysics* **612** (2018) A1.
- [18] S.S. Wilks, *The Large-Sample Distribution of the Likelihood Ratio for Testing Composite Hypotheses*, *The Annals of Mathematical Statistics* **9** (1938) 60.
- [19] H. Akaike, *Akaike's information criterion*, in *International encyclopedia of statistical science*, pp. 25–25, Springer (2011).

Full Author List: CTAO-LST Project

K. Abe¹, S. Abe², A. Abhishek³, F. Acero^{4,5}, A. Aguasca-Cabot⁶, I. Agudo⁷, C. Alispach⁸, D. Ambrosino⁹, F. Ambrosino¹⁰, L. A. Antonelli¹⁰, C. Aramo⁹, A. Arbet-Engels¹¹, C. Arcaro¹², T.T.H. Arnesen¹³, K. Asano², P. Aubert¹⁴, A. Baktash¹⁵, M. Balbo⁸, A. Bamba¹⁶, A. Baquero Larriva^{17,18}, V. Barbosa Martins¹⁹, U. Barres de Almeida²⁰, J. A. Barrio¹⁷, L. Barrios Jiménez¹³, I. Batkovic¹², J. Baxter², J. Becerra González¹³, E. Bernardini¹², J. Bernete²¹, A. Bertl¹¹, C. Bigongiari¹⁰, E. Bissaldi²², O. Blanch²³, G. Bonoli²⁴, P. Bordas⁶, G. Borkowski²⁵, A. Briscioli²⁶, G. Brunelli^{27,28}, J. Bucés¹⁷, A. Bulgarelli²⁷, M. Bunse²⁹, I. Burelli³⁰, L. Burmistrov³¹, M. Cardillo³², S. Caroff¹⁴, A. Carosi¹⁰, R. Carraro¹⁰, M. S. Carrasco²⁶, F. Cassol²⁶, D. Cerasole³³, G. Ceribella¹¹, A. Cerviño Cortez¹⁷, Y. Chai¹¹, K. Cheng², A. Chivassá^{34,35}, M. Chikawa², G. Chon¹¹, L. Chytka³⁶, G. M. Ciccari^{37,38}, A. Cifuentes²¹, J. L. Contreras¹⁷, J. Cortina²¹, H. Costantini²⁶, M. Croisnancier²³, M. Dalchenko³¹, P. Da Vela²⁷, F. Dazzi¹⁰, A. De Angelis¹², M. de Bony de Lavergne³⁹, R. Del Burgo⁹, C. Delgado²¹, J. Delgado Mengual⁴⁰, M. Dellaiera¹⁴, D. della Volpe³¹, B. De Lotto³⁰, L. Del Peral⁴¹, R. de Menezes³⁴, G. De Palma²², C. Díaz²¹, A. Di Piano²⁷, F. Di Piero³⁴, R. Di Tria³³, L. Di Venere⁴², D. Dominis Prester⁴³, A. Donini¹⁰, D. Dorner⁴⁴, M. Doró¹², L. Eisenberger⁴⁴, D. Elsässer⁴⁵, G. Emery²⁶, L. Feligioni²⁶, F. Ferrarotto⁴⁶, A. Fiasson^{14,47}, L. Foffano³², F. Frías García-Lago¹³, S. Fröse⁴⁵, Y. Fukazawa⁴⁸, S. Galozzi¹⁰, R. García López¹³, S. García Soto²¹, C. Gasbarra⁴⁹, D. Gasparrini⁴⁹, J. Giesbrecht Paiva²⁰, N. Giglietto²², F. Giordano³³, N. Godinovic⁵⁰, T. Gradetzke⁴⁵, R. Grau²³, L. Greaux¹⁹, D. Green¹¹, J. Green¹¹, S. Gunji⁵¹, P. Günther⁴⁴, J. Hackfeld¹⁹, D. Hadasch², A. Hahn¹¹, M. Hashizume⁴⁸, T. Hassan²¹, K. Hayashi^{52,2}, L. Heckmann^{11,53}, M. Heller³¹, J. Herrera Llorente¹³, K. Hirotani², D. Hoffmann²⁶, D. Horns¹⁵, J. Houles²⁶, M. Hrabovsky³⁶, D. Hrupec⁵⁴, D. Hui^{55,2}, M. Iarlori⁵⁶, R. Imazawa⁴⁸, T. Inada², Y. Inoue^{57,2}, K. Ioka⁵⁸, M. Iori⁴⁶, T. Itokawa², A. Iuliano⁹, J. Jahanvi³⁰, I. Jimenez Martinez¹¹, J. Jimenez Quiles²³, I. Jorge Rodrigo²¹, J. Juryssek⁵⁹, M. Kagaya^{52,2}, O. Kalashev⁶⁰, V. Karas⁶¹, H. Katagiri⁶², D. Kerszberg^{23,63}, M. Kherlakian¹⁹, T. Kiyomoto⁶⁴, Y. Kobayashi², K. Kohri⁶⁵, A. Kong², P. Kornecki⁷, H. Kubo², J. Kushida¹, B. Lacave³¹, M. Lainez¹⁷, G. Lamanna¹⁴, A. Lamastra¹⁰, L. Lemoigne¹⁴, M. Linhoff⁴⁵, S. Lombardi¹⁰, F. Longo⁶⁶, R. López-Coto⁷, M. López-Moya¹⁷, A. López-Oramas¹³, S. Loporchio³³, A. Lorini³, J. Lozano Bahilo⁴¹, F. Lucarelli¹⁰, H. Luciano⁶⁶, P. L. Luque-Escamilla⁶⁷, P. Majumdar^{68,2}, M. Makariev⁶⁹, M. Mallamaci^{37,38}, D. Manda⁵⁹, M. Manganaro⁴³, D. K. Maniadas¹⁰, G. Manicò³⁸, K. Mannheim⁴⁴, S. Marchesi^{28,27,70}, F. Marini¹², M. Mariotti¹², P. Marquet⁷¹, G. Marsella^{38,37}, J. Martí⁶⁷, O. Martinez^{72,73}, G. Martínez²¹, M. Martínez²³, A. Mas-Aguilar¹⁷, M. Massa³, G. Maurin¹⁴, D. Mazin^{2,11}, J. Méndez-Gallego⁷, S. Menon^{10,74}, E. Mestre Guillen⁷⁵, D. Miceli¹², T. Miener¹⁷, J. M. Miranda⁷², R. Mirzoyan¹¹, M. Mizote⁷⁶, T. Mizuno⁴⁸, M. Molero Gonzalez¹³, E. Molina¹³, T. Montaruli³¹, A. Moralejo²³, D. Morcuende⁷, A. Moreno Ramos⁷², A. Morselli⁴⁹, V. Moya¹⁷, H. Muraishi⁷⁷, S. Nagataki⁷⁸, T. Nakamori⁵¹, C. Nanci²⁷, A. Neronov⁶⁰, D. Nieto Castaño¹⁷, M. Nieves Rosillo¹³, L. Nikolice³, K. Nishijima¹, K. Noda^{57,2}, D. Nosek⁷⁹, V. Novotny⁷⁹, S. Nozaki², M. Ohishi², Y. Ohtani², T. Oka⁸⁰, A. Okumura^{81,82}, R. Orito⁸³, L. Orsini³, J. Otero-Santos⁷, P. Ottaviani⁸⁴, M. Palatiello¹⁰, G. Panebianco²⁷, D. Paneque¹¹, F. R. Pantaleo²², R. Paoletti³, J. M. Paredes⁶, M. Pech^{59,36}, M. Pecimotika²³, M. Peresano¹¹, F. Pfeifle⁴⁴, E. Pietropaolo⁵⁶, M. Pihc⁶, G. Pirola¹¹, C. Plard¹⁴, F. Podobnik³, M. Polo²¹, E. Prandini¹², M. Prouza⁵⁹, S. Rainò³³, R. Rando¹², W. Rhode⁴⁵, M. Ribó⁶, V. Rizzi⁵⁰, G. Rodríguez Fernandez⁴⁹, M. D. Rodríguez Frias⁴¹, P. Romano²⁴, A. Roy⁴⁸, A. Ruina¹², E. Ruiz-Velasco¹⁴, T. Saito², S. Sakurai², D. A. Sanchez¹⁴, H. Sanó^{85,2}, T. Šarić³⁰, Y. Sato⁸⁶, F. G. Saturni¹⁰, V. Savchenko⁶⁰, F. Schiavone³³, B. Schleicher⁴⁴, F. Schmuckermaier¹¹, F. Schussler³⁹, T. Schweizer¹¹, M. Seglar Arroyo²³, T. Siegen⁴⁴, G. Silvestri¹², A. Simongini^{10,74}, J. Sitarek²⁵, V. Sliusar⁸, I. Sofía³⁴, A. Stamerra¹⁰, J. Strišković⁵⁴, M. Strzys², Y. Suda⁴⁸, A. Sunny^{10,74}, H. Tajima⁸¹, M. Takahashi⁸¹, J. Takata², R. Takeishi², P. H. T. Tam², S. J. Tanaka⁸⁶, D. Tateishi⁹⁴, T. Tavernier⁵⁹, P. Temnikov⁶⁹, Y. Terada⁶⁴, K. Terachi⁸⁰, T. Terzie⁴³, M. Teshima^{11,2}, M. Tluczykont¹⁵, F. Tokana⁵¹, T. Tomura², D. F. Torres⁷⁵, F. Tramonti³, P. Travnicek⁵⁹, G. Tripodo³⁸, A. Tutone¹⁰, M. Vacula³⁶, J. van Scherpenberg¹¹, M. Vázquez Acosta¹³, S. Ventura³, S. Vercellone²⁴, G. Verna³, I. Viale¹², A. Vigniano³⁰, C. F. Vigorito^{34,35}, E. Visentin^{34,35}, V. Vitale⁴⁹, V. Voitsekovskiy³¹, G. Voutsinas³¹, I. Vovk², T. Vuillaume¹⁴, R. Walter⁸, L. Wan², J. Wójcicki²⁵, T. Yamamoto⁷⁶, R. Yamazaki⁸⁶, Y. Yao¹, P. K. H. Yeung², T. Yoshida⁶², T. Yoshikoshi², W. Zhang⁷⁵, The CTAO-LST Project

¹Department of Physics, Tokai University, 4-1-1, Kita-Kaname, Hiratsuka, Kanagawa 259-1292, Japan. ²Institute for Cosmic Ray Research, University of Tokyo, 5-1-5, Kashiwa-no-ha, Kashiwa, Chiba 277-8582, Japan. ³INFN and Università degli Studi di Siena, Dipartimento di Scienze Fisiche, della Terra e dell'Ambiente (DSFTA), Sezione di Fisica,

Via Roma 56, 53100 Siena, Italy. ⁴Université Paris-Saclay, Université Paris Cité, CEA, CNRS, AIM, F-91191 Gif-sur-Yvette Cedex, France. ⁵FSLAC IRL 2009, CNRS/IAAC, La Laguna, Tenerife, Spain. ⁶Departament de Física Quàntica i Astrofísica, Institut de Ciències del Cosmos, Universitat de Barcelona, IECC-UB, Martí i Franquès, 1, 08028, Barcelona, Spain. ⁷Instituto de Astrofísica de Andalucía-CSIC, Glorieta de la Astronomía s/n, 18008, Granada, Spain. ⁸Department of Astronomy, University of Geneva, Chemin d'Ecogia 16, CH-1290 Versoix, Switzerland. ⁹INFN Sezione di Napoli, Via Cintia, ed. G, 80126 Napoli, Italy. ¹⁰INAF - Osservatorio Astronomico di Roma, Via di Frascati 33, 00040, Monteporzio Catone, Italy. ¹¹Max-Planck-Institut für Physik, Boltzmannstraße 8, 85748 Garching bei München. ¹²INFN Sezione di Padova and Università degli Studi di Padova, Via Marzolo 8, 35131 Padova, Italy. ¹³Instituto de Astrofísica de Canarias and Departamento de Astrofísica, Universidad de La Laguna, C. Via Láctea, s/n, 38205 La Laguna, Santa Cruz de Tenerife, Spain. ¹⁴Univ. Savoie Mont Blanc, CNRS, Laboratoire d'Annecy de Physique des Particules - IN2P3, 74000 Annecy, France. ¹⁵Universität Hamburg, Institut für Experimentalphysik, Luruper Chaussee 149, 22761 Hamburg, Germany. ¹⁶Graduate School of Science, University of Tokyo, 7-3-1 Hongo, Bunkyo-ku, Tokyo 113-0033, Japan. ¹⁷IPARCOS-UCM, Instituto de Física de Partículas y del Cosmos, and EMFTEL Department, Universidad Complutense de Madrid, Plaza de Ciencias, 1. Ciudad Universitaria, 28040 Madrid, Spain. ¹⁸Faculty of Science and Technology, Universidad del Azuay, Cuenca, Ecuador. ¹⁹Institut für Theoretische Physik, Lehrstuhl IV: Plasma-Astroteilchenphysik, Ruhr-Universität Bochum, Universitätsstraße 150, 44801 Bochum, Germany. ²⁰Centro Brasileiro de Pesquisas Físicas, Rua Xavier Sigaud 150, RJ 22290-180, Rio de Janeiro, Brazil. ²¹CIEMAT, Avda. Complutense 40, 28040 Madrid, Spain. ²²INFN Sezione di Bari and Politecnico di Bari, via Orabona 4, 70124 Bari, Italy. ²³Institut de Física d'Altes Energies (IFAE), The Barcelona Institute of Science and Technology, Campus UAB, 08193 Bellaterra (Barcelona), Spain. ²⁴INAF - Osservatorio Astronomico di Brera, Via Brera 28, 20121 Milano, Italy. ²⁵Faculty of Physics and Applied Informatics, University of Lodz, ul. Pomorska 149-153, 90-236 Lodz, Poland. ²⁶Aix Marseille Univ. CNRS/IN2P3, CPPM, Marseille, France. ²⁷INAF - Osservatorio di Astrofisica e Scienza dello spazio di Bologna, Via Piero Gobetti 93/3, 40129 Bologna, Italy. ²⁸Dipartimento di Fisica e Astronomia (DIFA) Augusto Righi, Università di Bologna, via Gobetti 93/2, I-40129 Bologna, Italy. ²⁹Lamarr Institute for Machine Learning and Artificial Intelligence, 44227 Dortmund, Germany. ³⁰INFN Sezione di Trieste and Università degli studi di Udine, via delle scienze 206, 33100 Udine, Italy. ³¹University of Geneva - Département de physique nucléaire et corpusculaire, 24 Quai Ernest Ansermet, 1211 Genève 4, Switzerland. ³²INAF - Istituto di Astrofisica e Planetologia Spaziali (IAPS), Via del Fosso del Cavaliere 100, 00133 Roma, Italy. ³³INFN Sezione di Bari and Università di Bari, via Orabona 4, 70126 Bari, Italy. ³⁴INFN Sezione di Torino, via P. Giuria 1, 10125 Torino, Italy. ³⁵Dipartimento di Fisica - Università degli Studi di Torino, Via Pietro Giuria 1 - 10125 Torino, Italy. ³⁶Palacky University Olomouc, Faculty of Science, 17. listopadu 1192/12, 771 46 Olomouc, Czech Republic. ³⁷Dipartimento di Fisica e Chimica 'E. Segrè' Università degli Studi di Palermo, via delle Scienze, 90128 Palermo. ³⁸INFN Sezione di Catania, Via S. Sofia 64, 95123 Catania, Italy. ³⁹IRFU, CEA, Université Paris-Saclay, Bât 141, 91191 Gif-sur-Yvette, France. ⁴⁰Port d'Informació Científica, Edifici D, Carrer de l'Albareda, 08193 Bellaterra (Cerdanyola del Vallès), Spain. ⁴¹University of Alcalá UAH, Departamento de Physics and Mathematics, Pza. San Diego, 28801, Alcalá de Henares, Madrid, Spain. ⁴²INFN Sezione di Bari, via Orabona 4, 70125, Bari, Italy. ⁴³University of Rijeka, Department of Physics, Radmile Matejčić 2, 51000 Rijeka, Croatia. ⁴⁴Institute for Theoretical Physics and Astrophysics, Universität Würzburg, Campus Hubland Nord, Emil-Fischer-Str. 31, 97074 Würzburg, Germany. ⁴⁵Department of Physics, TU Dortmund University, Otto-Hahn-Str. 4, 44227 Dortmund, Germany. ⁴⁶INFN Sezione di Roma La Sapienza, P.le Aldo Moro, 2 - 00185 Rome, Italy. ⁴⁷ILANCE, CNRS - University of Tokyo International Research Laboratory, University of Tokyo, 5-1-5 Kashiwa-no-Ha Kashiwa City, Chiba 277-8582, Japan. ⁴⁸Physics Program, Graduate School of Advanced Science and Engineering, Hiroshima University, 1-3-1 Kagamiyama, Higashi-Hiroshima City, Hiroshima, 739-8526, Japan. ⁴⁹INFN Sezione di Roma Tor Vergata, Via della Ricerca Scientifica 1, 00133 Rome, Italy. ⁵⁰University of Split, FESB, R. Boškovića 32, 21000 Split, Croatia. ⁵¹Department of Physics, Yamagata University, 1-4-12 Kojirakawa-machi, Yamagata-shi, 990-8560, Japan. ⁵²Sendai College, National Institute of Technology, 4-16-1 Ayashi-Chuo, Aoba-ku, Sendai city, Miyagi 989-3128, Japan. ⁵³Université Paris Cité, CNRS, Astroparticule et Cosmologie, F-75013 Paris, France. ⁵⁴Josip Juraj Strossmayer University of Osijek, Department of Physics, Trg Ljudevita Gaja 6, 31000 Osijek, Croatia. ⁵⁵Department of Astronomy and Space Science, Chungnam National University, Daejeon 34134, Republic of Korea. ⁵⁶INFN Dipartimento di Scienze Fisiche e Chimiche - Università degli Studi dell'Aquila and Gran Sasso Science Institute, Via Vetoio 1, Viale Crispi 7, 67100 L'Aquila, Italy. ⁵⁷Chiba University, 1-33, Yayoi-cho, Inage-ku, Chiba-shi, Chiba, 263-8522 Japan. ⁵⁸Kitashirakawa Oiwa-kecho, Sakyo Ward, Kyoto, 606-8502, Japan. ⁵⁹FZU - Institute of Physics of the Czech Academy of Sciences, Na Slovance 1999/2, 182 21 Praha 8, Czech Republic. ⁶⁰Laboratory for High Energy Physics, École Polytechnique Fédérale, CH-1015 Lausanne, Switzerland. ⁶¹Astronomical Institute of the Czech Academy of Sciences, Boční II 1401 - 14100 Prague, Czech Republic. ⁶²Faculty of Science, Ibaraki University, 2 Chome-1-1 Bunkyo, Mito, Ibaraki 310-0056, Japan. ⁶³Sorbonne Université, CNRS/IN2P3, Laboratoire de Physique Nucléaire et de Hautes Energies, LPNHE, 4 place Jussieu, 75005 Paris, France. ⁶⁴Graduate School of Science and Engineering, Saitama University, 255 Simo-Ohkubo, Sakura-ku, Saitama city, Saitama 338-8570, Japan. ⁶⁵Institute of Particle and Nuclear Studies, KEK (High Energy Accelerator Research Organization), 1-1 Oho, Tsukuba, 305-0801, Japan. ⁶⁶INFN Sezione di Trieste and Università degli Studi di Trieste, Via Valerio 2 I, 34127 Trieste, Italy. ⁶⁷Escuela Politécnica Superior de Jaén, Universidad de Jaén, Campus Las Lagunillas s/n, Edif. A3, 23071 Jaén, Spain. ⁶⁸Saha Institute of Nuclear Physics, A CI of Homi Bhabha National Institute, Kolkata 700064, West Bengal, India. ⁶⁹Institute for Nuclear Research and Nuclear Energy, Bulgarian Academy of Sciences, 72 boul. Tsarigradsko chaussee, 1784 Sofia, Bulgaria. ⁷⁰Department of Physics and Astronomy, Clemson University, Kinard Lab of Physics, Clemson, SC 29634, USA. ⁷¹Institut de Física d'Altes Energies (IFAE), The Barcelona Institute of Science and Technology, Campus UAB, 08193 Bellaterra (Barcelona), Spain. ⁷²Grupo de Electronica, Universidad Complutense de Madrid, Av. Complutense s/n, 28040 Madrid, Spain. ⁷³E.S.CC. Experimentales y Tecnológica (Departamento de Biología y Geología, Física y Química Inorgánica) - Universidad Rey Juan Carlos. ⁷⁴Macroarea di Scienze MMFFNN, Università di Roma Tor Vergata, Via della Ricerca Scientifica 1, 00133 Rome, Italy. ⁷⁵Institute of Space Sciences (ICE, CSIC), and Institut d'Estudis Espacials de Catalunya (IEEC), and Institut Catalana de Recerca i Estudis Avançats (ICREA), Campus UAB, Carrer de Can Magrans, s/n 08193 Bellaterra, Spain. ⁷⁶Department of Physics, Konan University, 8-9-1 Okamoto, Higashinada-ku Kobe 658-8501, Japan. ⁷⁷School of Allied Health Sciences, Kitasato University, Sagamihara, Kanagawa 228-8555, Japan. ⁷⁸RIKEN, Institute of Physical and Chemical Research, 2-1 Hiroswawa, Wako, Saitama, 351-0198, Japan. ⁷⁹Charles University, Institute of Particle and Nuclear Physics, V Holešovičkách 2, 180 00 Prague 8, Czech Republic. ⁸⁰Division of Physics and Astronomy, Graduate School of Science, Kyoto University, Sakyo-ku, Kyoto, 606-8502, Japan. ⁸¹Institute for Space-Earth Environmental Research, Nagoya University, Chikusa-ku, Nagoya 464-8601, Japan. ⁸²Kobayashi-Maskawa Institute (KMI) for the Origin of Particles and the Universe, Nagoya University, Chikusa-ku, Nagoya 464-8602, Japan. ⁸³Graduate School of Technology, Industrial and Social Sciences, Tokushima University, 2-1 Minamijosanjima, Tokushima, 770-8506, Japan. ⁸⁴INFN Sezione di Pisa, Edificio C - Polo Fibonaccii, Largo Bruno Pontecorvo 3, 56127 Pisa, Italy. ⁸⁵Gifu University, Faculty of Engineering, 1-1 Yanagido, Gifu 501-1193, Japan. ⁸⁶Department of Physical Sciences, Aoyama Gakuin University, Fuchinobe, Sagamihara, Kanagawa, 252-5258, Japan.

Acknowledgments

We gratefully acknowledge financial support from the following agencies and organisations: Conselho Nacional de Desenvolvimento Científico e Tecnológico (CNPq), Fundação de Amparo à Pesquisa do Estado do Rio de Janeiro (FAPERJ), Fundação de Amparo à Pesquisa do Estado de São Paulo (FAPESP), Fundação de Apoio à Ciência, Tecnologia e Inovação do Paraná - Fundação Araucária, Ministry of Science, Technology, Innovations and Communications (MCTIC), Brasil; Ministry of Education and Science, National RI Roadmap Project DOI-153/28.08.2018, Bulgaria; Croatian Science Foundation (HrZZ) Project IP-2022-10-4595, Rudjer Boskovic Institute, University of Osijek, University of Rijeka, University of Split, Faculty of Electrical Engineering, Mechanical Engineering and Naval Architecture, University of Zagreb, Faculty of Electrical Engineering and Computing, Croatia; Ministry of Education, Youth and Sports, MEYS LM2023047, EU/MEYS CZ.02.1.01/0.0/0.0/16_013/0001403, CZ.02.1.01/0.0/0.0/18_046/0016007, CZ.02.1.01/0.0/0.0/16_019/0000754, CZ.02.01.01/00/22_008/0004632 and CZ.02.01.01/00/23_015/0008197 Czech Republic; CNRS-IN2P3, the French Programme d'investissements d'avenir and the Enigmass Labex. This work has been done thanks to the facilities offered by the Univ. Savoie Mont Blanc - CNRS/IN2P3 MUST computing center, France; Max Planck Society, German Bundesministerium für Bildung und Forschung (Verbundforschung / ErUM), Deutsche Forschungsgemeinschaft (SFBs 876 and 1491), Germany; Istituto Nazionale di Astrofisica (INAF), Istituto Nazionale di Fisica Nucleare (INFN), Italian Ministry for University and Research (MUR), and the financial support from the European Union - Next Generation EU under the project IR0000012 - CTA+ (CUP C53C22000430006), announcement N.3264 on 28/12/2021: "Rafforzamento e creazione di IR nell'ambito del Piano Nazionale di Ripresa e Resilienza (PNRR)"; ICRR, University of Tokyo, JSPS, MEXT, Japan; JST SPRING - JP-MJSP2108; Narodowe Centrum Nauki, grant number 2023/50/A/ST9/00254, Poland; The Spanish groups acknowledge the Spanish Ministry of Science and Innovation and the Spanish Research State Agency (AEI) through the government budget lines PGE2022/28.06.000X.711.04, 28.06.000X.411.01 and 28.06.000X.711.04 of PGE 2023, 2024 and 2025, and grants PID2019-104114RB-C31, PID2019-107847RB-C44, PID2019-104114RB-C32, PID2019-10510GB-C31, PID2019-104114RB-C33, PID2019-107847RB-C43, PID2019-107847RB-C42, PID2019-107988GB-C22, PID2021-124581OB-I00, PID2021-125331NB-I00, PID2022-136828NB-C41, PID2022-137810NB-C22, PID2022-138172NB-C41, PID2022-138172NB-C42, PID2022-138172NB-C43, PID2022-139117NB-C41, PID2022-139117NB-C42, PID2022-139117NB-C43, PID2022-139117NB-C44, PID2022-136828NB-C42, PDC2023-145839-I00 funded by the Spanish MCIN/AEI/10.13039/501100011033 and "and by ERDF/EU and NextGenerationEU PRTR; the "Centro de Excelencia Severo Ochoa" program through grants no. CEX2019-000920-S, CEX2020-001007-S, CEX2021-001131-S; the "Unidad de Excelencia María de Maeztu" program through grants no. CEX2019-000918-M, CEX2020-001058-M; the "Ramón y Cajal" program through grants RYC2021-032991-I funded by MICIN/AEI/10.13039/501100011033 and the European Union "NextGenerationEU"/PRTR and RYC2020-028639-I; the "Juan de la Cierva-Incorporación" program through grant no. IJC2019-040315-I and "Juan de la Cierva-formación" through grant JDC2022-049705-I. They also acknowledge the "Atracción de Talento" program of Comunidad de Madrid through grant no. 2019-T2/TIC-12900; the project "Tecnologías avanzadas para la exploración del universo y sus componentes" (PR47/21 TAU), funded by Comunidad de Madrid, by the Recovery, Transformation and Resilience Plan from the Spanish State, and by NextGenerationEU from the European Union through the Recovery and Resilience Facility; "MAD4SPACE: Desarrollo de

tecnologías habilitadoras para estudios del espacio en la Comunidad de Madrid" (TEC-2024/TEC-182) project funded by Comunidad de Madrid; the La Caixa Banking Foundation, grant no. LCF/BQ/PI21/11830030; Junta de Andalucía under Plan Complementario de I+D+I (Ref. AST22_0001) and Plan Andaluz de Investigación, Desarrollo e Innovación as research group FQM-322; Project ref. AST22_00001_9 with funding from NextGenerationEU funds; the "Ministerio de Ciencia, Innovación y Universidades" and its "Plan de Recuperación, Transformación y Resiliencia"; "Consejería de Universidad, Investigación e Innovación" of the regional government of Andalucía and "Consejo Superior de Investigaciones Científicas", Grant CNS2023-144504 funded by MICIU/AEI/10.13039/501100011033 and by the European Union NextGenerationEU/PRTR, the European Union's Recovery and Resilience Facility-Next Generation, in the framework of the General Invitation of the Spanish Government's public business entity Red.es to participate in talent attraction and retention programmes within Investment 4 of Component 19 of the Recovery, Transformation and Resilience Plan; Junta de Andalucía under Plan Complementario de I+D+I (Ref. AST22_00001), Plan Andaluz de Investigación, Desarrollo e Innovación (Ref. FQM-322). "Programa Operativo de Crecimiento Inteligente" FEDER 2014-2020 (Ref. ESFRI-2017-IAC-12), Ministerio de Ciencia e Innovación, 15% co-financed by Consejería de Economía, Industria, Comercio y Conocimiento del Gobierno de Canarias; the "CERCA" program and the grants 2021SGR00426 and 2021SGR00679, all funded by the Generalitat de Catalunya; and the European Union's NextGenerationEU (PRTR-C17.11). This research used the computing and storage resources provided by the Port d'Informació Científica (PIC) data center. State Secretariat for Education, Research and Innovation (SERI) and Swiss National Science Foundation (SNSF), Switzerland; The research leading to these results has received funding from the European Union's Seventh Framework Programme (FP7/2007-2013) under grant agreements No 262053 and No 317446; This project is receiving funding from the European Union's Horizon 2020 research and innovation programs under agreement No 676134; ESCAPE - The European Science Cluster of Astronomy & Particle Physics ESFRI Research Infrastructures has received funding from the European Union's Horizon 2020 research and innovation programme under Grant Agreement no. 824064.

We would like to thank the Instituto de Astrofísica de Canarias for the excellent working conditions at the Observatorio del Roque de los Muchachos in La Palma. The financial support of the German BMBF, MPG and HGF; the Italian INFN and INAF; the Swiss National Fund SNF; the grants PID2019-107988GB-C22, PID2022-136828NB-C41, PID2022-137810NB-C22, PID2022-138172NB-C41, PID2022-138172NB-C42, PID2022-138172NB-C43, PID2022-139117NB-C41, PID2022-139117NB-C42, PID2022-139117NB-C43, PID2022-139117NB-C44, CNS2023-144504 funded by the Spanish MCIN/AEI/ 10.13039/501100011033 and "ERDF A way of making Europe; the Indian Department of Atomic Energy; the Japanese ICRR, the University of Tokyo, JSPS, and MEXT; the Bulgarian Ministry of Education and Science, National RI Roadmap Project DO1-400/18.12.2020 and the Academy of Finland grant nr. 320045 is gratefully acknowledged. This work was also been supported by Centros de Excelencia "Severo Ochoa" y Unidades "María de Maeztu" program of the Spanish MCIN/AEI/ 10.13039/501100011033 (CEX2019-000920-S, CEX2019-000918-M, CEX2021-001131-S) and by the CERCA institution and grants 2021SGR00426 and 2021SGR00773 of the Generalitat de Catalunya; by the Croatian Science Foundation (HrZZ) Project IP-2022-10-4595 and the University of Rijeka Project uniri-prirod-18-48; by the Deutsche Forschungsgemeinschaft (SFB1491) and by the Lamar-Institute for Machine Learning and Artificial Intelligence; by the Polish Ministry Of Education and Science grant No. 2021/WK/08; and by the Brazilian MCTIC, CNPq and FAPERJ.